Turkish Journal of Civil Engineering, 2027, xxxx-xxxx, Paper xxx, ***Technical Note***

Strength Behavior and Microstructure Characterization of Self-Consolidating Concrete with Sintered Fly Ash Coarse Aggregates

Pawan KUMAR[1]
Dinakar PASLA[2*]
Jothi Saravanan THIYAGARAJAN[3]

ABSTRACT

Self-consolidating concrete (SCC) made with sintered fly ash aggregates (SFAA) was investigated for its compressive strength and microstructural properties. Even with significant additions of mineral admixtures such as silica fume (SF) and metakaolin (MK) and 100% SFAA, the formulated SCC demonstrated compressive strength satisfying the minimum requirements for structural lightweight concrete, in accordance with established standards such as those recommended by the ACI 318-19, BS EN 206-1 and Eurocode 2 after 28 and 90 days of curing. Strength development was corroborated through SEM and EDS analysis, while non-destructive methods, including rebound hammer and ultrasonic pulse velocity (UPV), confirmed the enhancements in compressive strength.

Keywords: Sintered fly ash aggregates, self-consolidating concrete, mineral admixtures, microstructural investigation.

1. INTRODUCTION

Integrating self-consolidating concrete (SCC) with sintered fly ash aggregates (SFAA) offers significant benefits for construction projects by reducing structural dead load, ensuring high-quality finishes, enabling efficient placement, and enhancing strength and durability. Lightweight SCC provides numerous advantages in building construction, including reduced permanent loads, the potential for smaller foundation sizes, material

---

Note:
- This paper was received on February 02, 2026 and accepted for publication by the Editorial Board on July 16, 2026.
- Discussions on this paper will be accepted by xxxxxxx xx, xxxx.

- https://doi.org/

1 School of Civil Engineering, Lovely Professional University, Punjab, India
pawan.34551@lpu.co.in - https://orcid.org/0009-0001-7530-8881

2 School of Infrastructure, Indian Institute of Technology, Bhubaneswar, India
pdinakar@iitbbs.ac.in - https://orcid.org/0000-0003-2524-2404

3 School of Infrastructure, Indian Institute of Technology, Bhubaneswar, India
tjs@iitbbs.ac.in - https://orcid.org/0009-0000-6620-4944

* Corresponding author

savings, enhanced fire resistance, and improved thermal insulation, among other benefits. The properties and proportion of fillers, fines, and superplasticizers significantly influence mortar quality, essential for achieving the desired workability and strength in SCC (Kumar et al., 2024a). SFAA is usually created by combining fly ash with clay using a pelletizer with appropriate water. The resulting green pellets are then subjected to a controlled sintering process on slowly moving horizontal grates at a regulated temperature (Kumar et al., 2023a; Nadesan & Dinakar, 2017; Rawat & Pasla, 2024). Silica fume (SF) is a by-product recovered from producing alloys containing silicon or ferrosilicon and is usually composed of over 85% amorphous silica (Naito et al., 2020). Metakaolin (MK) is a very reactive substance formed by heating kaolinite. MK can potentially enhance the loadbearing capacities and reduce contraction/shrinkage induced by its particle packing (Güneyisi et al., 2012; Tejas & Pasla, 2023a, 2023b).

These fillers enhance the hydration process of mortar paste through a nucleation effect, increasing the density and thickness of the calcium silicate hydrate (C-S-H) layer. The study aims to develop structural-grade lightweight SCC with reduced density while ensuring the required fresh properties (flowability and passing ability) and sufficient mechanical strength for structural applications. A substantial body of literature is already available on SCC produced with conventional aggregates, and its fresh and hardened properties are well established. In contrast, the behavior of SCC incorporating artificial aggregates remains comparatively less explored, particularly in terms of achieving self-compacting characteristics while maintaining structural-grade strength. Therefore, the present study focuses on intra-group comparisons among SFAA-based mixtures to systematically evaluate the influence of SCMs on fresh, mechanical, and microstructural performance. This approach allows for a clearer understanding of the material behavior within the intended lightweight system. In addition, microstructural analysis was also performed to analyse microcracks and voids.

2. PROPERTIES OF MATERIALS AND EXPERIMENTAL PROCEDURE

The chemical composition of the raw materials was determined using XRF analysis, which indicated that both SF and MK contain significant amounts of SiO_2, with SF comprising 90.4% and MK 48.01%. The analysis further revealed that the SFAA are also rich in SiO_2, with a content approaching 60%. To complement the compositional analysis and address the reactivity aspect, the pozzolanic activity of SF and MK was evaluated through the Strength Activity Index (SAI) test as part of the preliminary investigation. The obtained SAI values exceeded 75%, thereby confirming the adequate pozzolanic reactivity of the materials used. Natural fine aggregates (NFA) primarily comprise silica, alumina, and trace amounts of other oxides. The particle size distribution curves of the binder used in this investigation are presented in Figure 1 (a).

SFAA has a specific gravity of 1.45 and a water absorption rate of 18%. Nine SCC mixes incorporating SFAA [4-8 mm and 8-12 mm] were developed, including one base SCC mix. The base SCC mix included 550 kg/m³ of 53-grade cement, 170 kg/m³ of water, 819 kg/m³ of NFA, and 377 kg/m³ of SFA, along with 0.8% of PCE-based MasterGlenium ACE 30UG. The w/b ratio (0.30) was maintained consistently, while cement was substituted with SF or MK at 7.5%, 10%, 12.5%, and 15% throughout the study (Table 1).

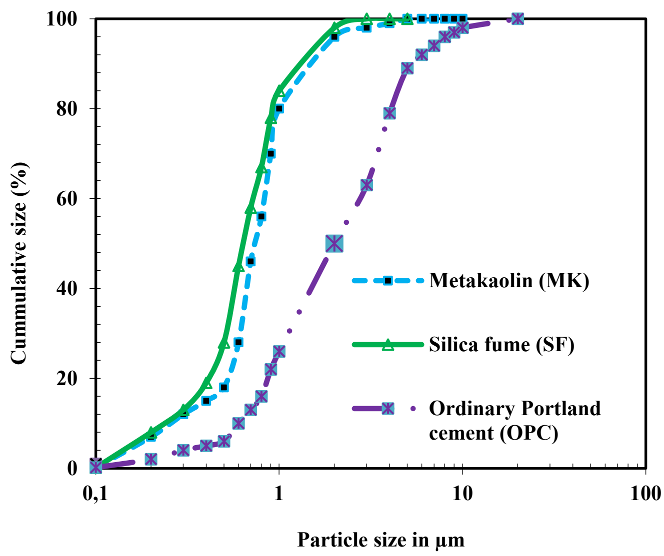

(a) Particle size distribution of the binders

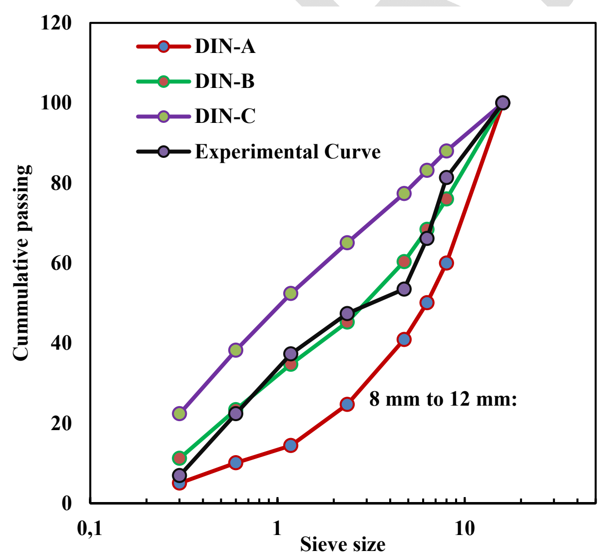

(b) Combined grading of used aggregates

Figure 1. Particle size distribution curve of the material used

The superplasticiser dosage was adjusted to regulate the slump flow (SF2) in the SCC mixes. The SCC mix notations included C-SFAA for the base mix, while the replacement level mixes were labelled as 7.5SF-SFAA, 10SF-SFAA, 12.5SF-SFAA, and 15SF-SFAA

Table 1. Mix proportion of the developed SFAA-based SCC mixes in kg/m³

Mix ID	PC	Water	MK	SF	SFAA		NFA	SP
					4–8 mm	8–12 mm		
	in (kg/m³)							in (%)
C-SFAA (Base)	550	170	-	-	136	241	819	0.8
7.5SF-SFAA	509	170	-	41	159	282	819	1
10SF-SFAA	495	170	-	55	158	281	816	1.1
12.5SF-SFAA	481	170	-	69	158	280	814	1.3
15SF-SFAA	468	170	-	83	157	280	811	1.4
7.5MK-SFAA	509	170	41	-	159	283	822	1.1
10MK-SFAA	495	170	55	-	159	283	821	1.2
12.5MK-SFAA	481	170	69	-	159	283	820	1.3
15MK-SFAA	468	170	83	-	159	282	819	1.5

for SF substitutions, and 7.5MK-SFAA, 10MK-SFAA, 12.5MK-SFAA, and 15MK-SFAA for MK replacements. The mix design and workability process followed the EFNARC standard (2005). The aggregate quantity was determined using the DIN grading curve [Figure 1(b)], and a two-stage mixing technique was employed to ensure proper blending of the SCC components. The selection of the DIN curve in the present study was based on its ability to provide a dense and continuous particle size distribution, which enhances particle packing. Improved packing density reduces void content and thereby supports the flowability and stability requirements of SCC when combined with an appropriate paste volume and admixtures. Furthermore, the adoption of the DIN grading curve is consistent with previous studies (Kumar et al., 2023b, 2024b; Nadesan & Pasala, 2018), where similar approaches have been successfully utilised for developing self-compacting and lightweight

Table 2. Details on specimen dimensions, curing durations, and relevant codes

Test (s) performed	Followed standard	Size of specimen (s)	Casted samples (Quantity)	Age of curing (Days)
1. Workability tests	EFNARC 2005	-	-	-
2. Compressive strength	IS 516-2021	Cubes (100*100*100 mm)	54	28 and 90
3. Rebound hammer	IS 13311(Part 2): 1992			
4. Ultrasonic pulse velocity	IS 13311-1-1991 Part-(1)			

concrete mixtures. After completing the mixing process, the fresh behaviour of the developed SCC mixes was assessed. Following the workability tests, compressive strength was measured using 100 mm × 100 mm × 100 mm cubic specimens (an average of 3 specimens) as per Indian Standard 516 (IS 516 Part 1/Sec 1, 2021) as presented in Table 2.

The SEM images were used to analyse microcracks and voids, while the EDS analysis was conducted to determine the chemical composition. The selected regions were obtained from fractured surfaces of tested specimens to ensure a realistic representation of the hydrated matrix. For each mix, multiple regions were analysed, and the reported EDS values represent averaged results from several points to minimise local variability and improve reliability. Furthermore, the structural integrity of the hardened SFAA-based SCC was assessed through rebound hammer and UPV tests.

3. OUTCOMES AND DISCUSSIONS

The measured slump flow values indicate that all developed SCC mixes possessed sufficient filling ability to flow under their own weight without external vibration. Although the slump flow values remained within the EFNARC recommended range (650-800 mm), a gradual reduction was observed with increasing incorporation of SCMs and SFAA (Table 3). This behaviour can be attributed primarily to the porous and rough surface texture of SFAA, which increases internal friction and absorbs part of the mixing water during the initial mixing stage. Furthermore, highly reactive SCMs such as SF and MK possess extremely fine particle sizes and high specific surface areas, resulting in increased water demand. Consequently, a slight variation in workability was observed while maintaining acceptable self-compacting characteristics (Ankur & Singh, 2024b, 2026a, 2026b).

The T_{500} flow time provides an indication of the rate at which concrete spreads and is directly related to the viscosity of the fresh mixture. The relatively higher T_{500} values (Table 3) recorded for some mixes indicate a controlled increase in viscosity rather than poor workability. The increased viscosity results from the combined influence of the higher surface area of SCM particles, improved particle packing, and the water absorption characteristics of SFAA. This increase in viscosity is advantageous because it reduces the likelihood of segregation while still allowing adequate flowability for placement.

Similarly, the V-funnel test reflects the flow resistance and viscosity stability of SCC. The slightly longer V-funnel flow times observed in SCC mixes containing SFAA and SCMs are consistent with the increased cohesiveness of the concrete. The porous structure of SFAA temporarily absorbs mixing water, while the ultrafine SCM particles enhance the cohesion of the cementitious matrix by filling voids between larger particles. As a result, the mixes exhibit improved stability and reduced bleeding without compromising their ability to flow through confined spaces. The measured V-funnel times therefore indicate an appropriate balance between fluidity and stability, which is essential for producing segregation-resistant SCC. The high-water absorption capacity of SFAA also contributes to an internal curing effect. During mixing, a portion of the water is absorbed into the pores of the LWA and is gradually released as hydration progresses. This controlled release of water helps maintain moisture within the cement paste, enhances hydration, and prevents rapid loss of workability. In the fresh state, this mechanism contributes to improved cohesiveness and minimises bleeding and segregation, despite the use of 100% SFAA.

The L-box test further demonstrates that the developed SCC mixes possess satisfactory passing ability. The obtained L-box ratios ranging from 0.86 to 0.97 (Table 3) exceed the minimum EFNARC requirement of 0.80, indicating that the concrete was capable of flowing through congested reinforcement without significant blocking. This finding is particularly significant because replacing conventional coarse aggregate entirely with SFAA could potentially increase interparticle friction due to its rougher surface texture. Nevertheless, the optimised paste volume together with the beneficial filler and lubricating effects of the SCMs successfully compensated for this tendency, allowing the mixtures to maintain excellent passing ability.

Overall, the combined interpretation of the slump flow, T_{500}, V-funnel, and L-box results demonstrates that the fresh-state performance of the developed SCC mixes is governed not only by compliance with EFNARC limits but also by the synergistic interaction between SFAA and SCMs. While SFAA increases water demand because of its porous structure, the optimised mix design and the incorporation of SCMs enhance particle packing, cohesion, and viscosity stability. These mechanisms enable the concrete to achieve an appropriate balance among filling ability, passing ability, flowability, and segregation resistance, thereby confirming the suitability of SFAA as a complete replacement for conventional coarse aggregate in structural self-compacting lightweight concrete.

Table 3. Fresh characteristics of the developed SCC

Mix ID	**T_{500} (sec)**	**Slump flow (mm)**	**V funnel (s)**	**L box test**	**Ensuring compliance with the EFNARC guidelines.**	**Density (Kg/m^3)**
C-SFAA (Base)	8	670	23	0.87	Yes	1990
7.5SF-SFAA	7	655	25	0.89		1938
10SF-SFAA	7	675	24	0.86		1920
12.5SF-SFAA	6	658	21	0.90		1903
15SF-SFAA	6	680	20	0.88		1885
7.5MK-SFAA	8	685	18	0.96		1944
10MK-SFAA	7	698	21	0.97		1928
12.5MK-SFAA	6	710	24	0.87		1913
15MK-SFAA	7	665	22	0.90		1897

After successfully meeting the required workability criteria, namely passing ability, filling ability, and flowability as shown in Table 3, an evaluation of strength after 28 and 90 days revealed that replacing up to 15% of mineral admixtures (SF or MK) with cement improved

Table 4. Experimental Outcomes of the SFAA-based SCC containing SCMs

Mix ID	Compressive strength						Rebound hammer						Ultrasonic pulse velocity					
	28 days	SD	Error	90 days	SD	Error	28 days	SD	Error	90 days	SD	Error	28 days	SD	Error	90 days	SD	Error
C-SFAA (Base)	47.53	1.68	0.97	55.45	1.52	0.98	35.62	1.42	0.86	44.65	0.95	0.55	3491	14.42	8.33	3880	16.56	9.56
7.5SF-SFAA	47.89	2.37	1.37	59.74	7.98	4.61	36.87	0.88	0.51	44.97	0.88	0.50	3512	9.54	5.51	3950	18.33	10.58
10SF-SFAA	49.13	2.96	1.71	59.85	1.82	1.05	38.97	1.17	0.67	45.75	0.79	0.46	3557	10.50	6.06	3980	12.17	7.02
12.5SF-SFAA	50.31	2.69	1.55	59.97	2.52	1.46	39.54	0.82	0.47	46.84	0.67	0.39	3636	11.37	6.57	4000	11.02	6.36
15SF-SFAA	52.01	1.03	0.59	61.77	1.61	0.93	40.21	0.77	0.44	47.02	0.67	0.38	3689	10.07	5.81	4350	22.81	13.17
7.5MK-SFAA	48.09	2.06	1.19	57.94	2.25	1.30	36.91	1.18	0.68	44.98	1.13	0.65	3587	13.23	7.64	3920	12.01	6.94
10MK-SFAA	50.1	2.28	1.32	62.81	1.78	1.03	39.41	1.07	0.62	46.4	0.95	0.55	3624	10.60	6.12	4020	12.12	7.00
12.5MK-SFAA	51.29	1.76	1.02	64.76	1.74	1.00	40.34	1.06	0.51	47.89	1.52	0.88	3687	11.50	6.64	4180	11.06	6.39
15MK-SFAA	53.67	2.30	1.33	65.74	1.74	1.00	41.57	1.00	0.57	49	1.33	0.77	3702	9.54	5.51	4250	11.00	6.35

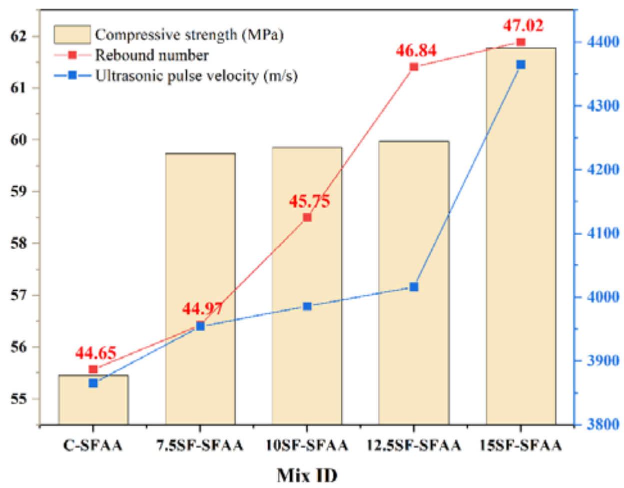

(a) Compressive strength, rebound number, and UPV results of SFAA-based SCC containing SF

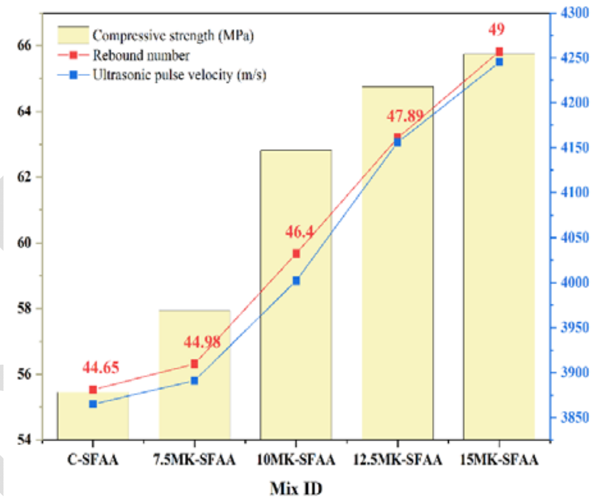

(b) Compressive strength, rebound number, and UPV results of SFAA-based SCC containing MK

Figure 2. Results obtained in this study

compressive strength compared to the base SCC mix (Figure 2). The particle size and shape of the fillers used significantly impacted the SCC. The recorded 90-days compressive strengths are listed in ascending order as 55.45 MPa, 59.74 MPa, 59.85 MPa, 59.97 MPa, 61.77 MPa, 57.94 MPa, 62.81 MPa, 64.76 MPa, and 65.74 MPa for SCC mixes C-SFAA, 7.5SF-SFAA, 10SF-SFAA, 12.5SF-SFAA, 15SF-SFAA, 7.5MK-SFAA, 10MK-SFAA, 12.5MK-SFAA, and 15MK-SFAA, respectively. The filler effect and pozzolanic reaction of SF or MK enhanced C-S-H formation and strengthened the bond between the aggregate and cement paste, ultimately leading to increased compressive strength (Gökçe et al., 2019; Kumar, Dinakar, et al., 2025; Kumar, Pasla, et al., 2025; Mermerdaş et al., 2012).

Additionally, the initial water absorption of SFAA (18%) in LWA-SCC mixes helps offset moisture loss in later stages, thereby supporting ongoing hydration. This finding also indicates that replacing coarse aggregates with SFAA in SCC can achieve a density reduction of up to 20%. Even with 100% artificial aggregates, the authors successfully achieved sufficient surface hardness (Table 4). A significant rise of around 4-5% was noted in the rebound number for SCC mix 12.5SF-SFAA and 15SF-SFAA, whereas incorporating 15% MK resulted in a 9% increase after 90 days compared to the base SCC mix (Figure 2). Despite variations in the UPV values of SCC mixes containing mineral admixtures compared to the base SCC mix C-SFAA, the structural integrity of the hardened SFAA-based SCC mixes remained unaffected, with most of the UPV values ranging between 3500 m/sec and 4500 m/sec, as shown in Figure 2. SF or MK also aids in developing a secondary C-S-H gel during hydration, as Ca (OH)2 interacts with silica, ultimately enhancing the overall performance. Furthermore, the residual SF or MK fills the voids between binder particles after completely consuming Ca (OH)2 (Kumar et al., 2024a; Kumar & Singh, 2023). Consequently, modifying the binder phase led to a decrease in pore count and a more refined microstructure.

4. MICROSTRUCTURAL EXAMINATION

The surface characteristics of SFAA-based SCC specimens were examined using a Merlin Compact Field Emission Scanning Electron Microscope. The microstructure of SCC mixes consists of a continuous network of C-S-H gel and several large C-H crystals within the matrix. The formation of a dense and continuous C-S-H structure within the matrix results from the pozzolanic reaction of SCMs, such as SF or MK. The structure becomes more compact and reinforced with time. SEM images of SFAA-based SCC show microscopic air voids formed due to the water absorption of the artificial aggregates.

The microstructural characterisation was further examined through SEM and EDS analyses to establish the relationship between hydration products, matrix densification, and the mechanical performance of the developed SCC mixes. SEM micrographs of 10SF-SFAA, 15SF-SFAA, 7.5MK-SFAA, 12.5MK-SFAA, and 15MK-SFAA are presented in Figures 3 and 5. The micrographs reveal a progressive refinement of the internal microstructure with increasing SF and MK content. Compared with the control mix (C-SFAA), the modified SCC mixtures exhibit a denser cementitious matrix, fewer micro voids, a more compact interfacial transition zone (ITZ), and a higher volume of hydration products. These improvements are particularly evident in the 15SF-SFAA and 15MK-SFAA mixtures, where the microstructure appears highly compact with a continuous network of C-S-H gel and minimal capillary pores. The enhanced packing effect of the ultrafine mineral admixtures, combined with their pozzolanic reactivity, promotes the formation of additional hydration products that effectively fill internal pores and discontinuities, resulting in a refined pore structure and stronger aggregate–paste bonding.

The improved hydration morphology observed in the SEM images is attributed to the dual action of SF and MK. Initially, their extremely fine particles provide a filler effect by occupying voids between cement grains, thereby enhancing particle packing density. Subsequently, both supplementary cementitious materials react with calcium hydroxide (CH) released during cement hydration through the pozzolanic reaction, consuming CH and producing additional secondary calcium silicate hydrate (C-S-H) gel. This secondary C-S-H fills capillary pores, reduces pore connectivity, strengthens the ITZ, and produces a more homogeneous and compact matrix. Consequently, the microstructure becomes less porous and more resistant to crack initiation and propagation, which directly contributes to the observed improvement in compressive strength.

The EDS analysis further validates these microstructural observations. The control mix (C-SFAA) exhibited the highest Ca/Si and Ca/(Si+Al) ratios of 5.040 and 3.32, respectively, followed by 7.5SF-SFAA (3.29 and 2.69), 10SF-SFAA (2.27 and 1.46), 12.5SF-SFAA (0.98 and 0.69), and 15SF-SFAA (0.151 and 0.109), as presented in Figure 6. A similar decreasing trend in the Ca/Si ratio was also observed for the MK-incorporated mixtures. The continuous reduction in the Ca/Si ratio with increasing SF and MK content indicates the progressive consumption of calcium hydroxide and the formation of silica-rich C-S-H gel through enhanced pozzolanic reactions. A lower Ca/Si ratio generally represents a more polymerised and chemically stable C-S-H structure with improved binding characteristics.

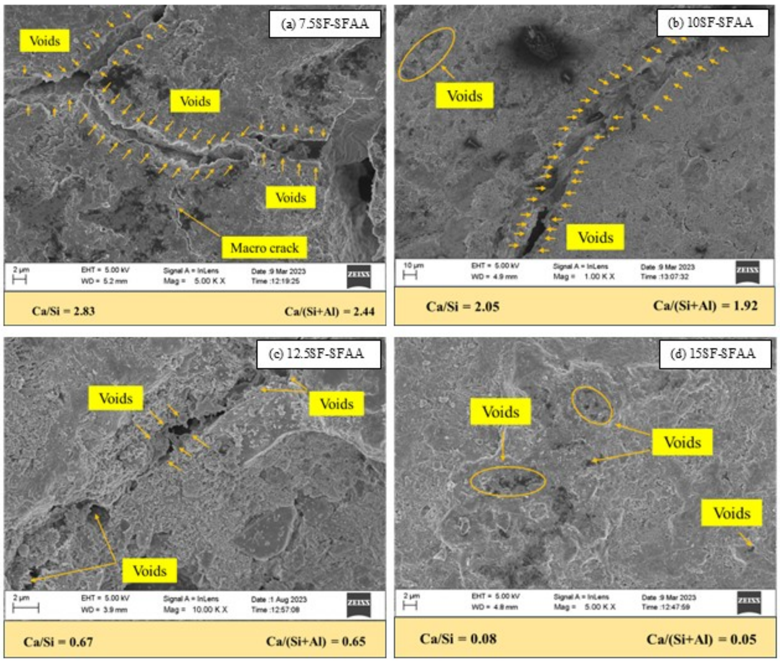

Figure 3. SEM images of SFAA-based SCC containing SF

The increased formation of secondary C-S-H simultaneously reduces the amount of free calcium hydroxide, which is comparatively weaker and more susceptible to deterioration, while producing a denser hydration matrix with significantly lower porosity.The reduction in pore volume and the development of a compact ITZ collectively enhance stress transfer between the lightweight sintered fly ash aggregate and the surrounding cement paste. The stronger aggregate–matrix bond minimises microcrack formation under compressive loading, thereby improving the overall mechanical performance of the SCC mixtures. Therefore, the lower Ca/Si ratios obtained from EDS analysis correlate well with the SEM observations of improved hydration morphology, refined pore structure, enhanced matrix densification, and strengthened ITZ development. These microstructural modifications explain the superior compressive strength achieved by the SCC mixtures containing higher proportions of silica fume and metakaolin. The inverse relationship between the Ca/Si ratio and compressive strength observed in the present investigation is consistent with previous studies, confirming that increased pozzolanic activity and greater C-S-H formation are the primary mechanisms responsible for the enhanced performance of the developed lightweight SCC mixtures (Ankur & Singh, 2024a).

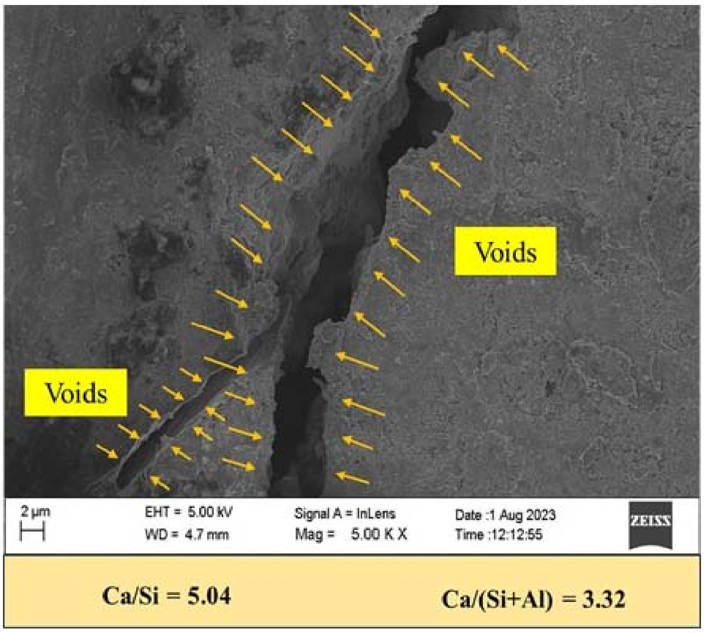

Figure 4. SEM images of base SCC mix C-SFAA

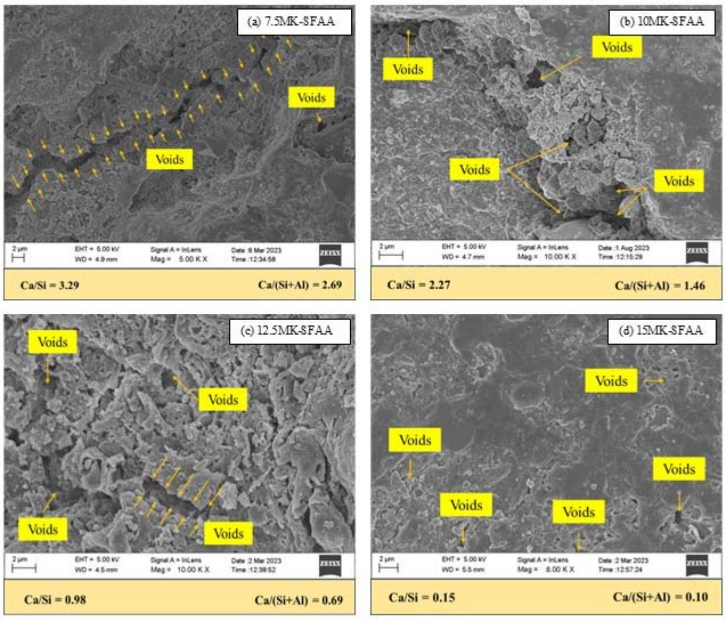

Figure 5. SEM images of SFAA-based SCC containing MK

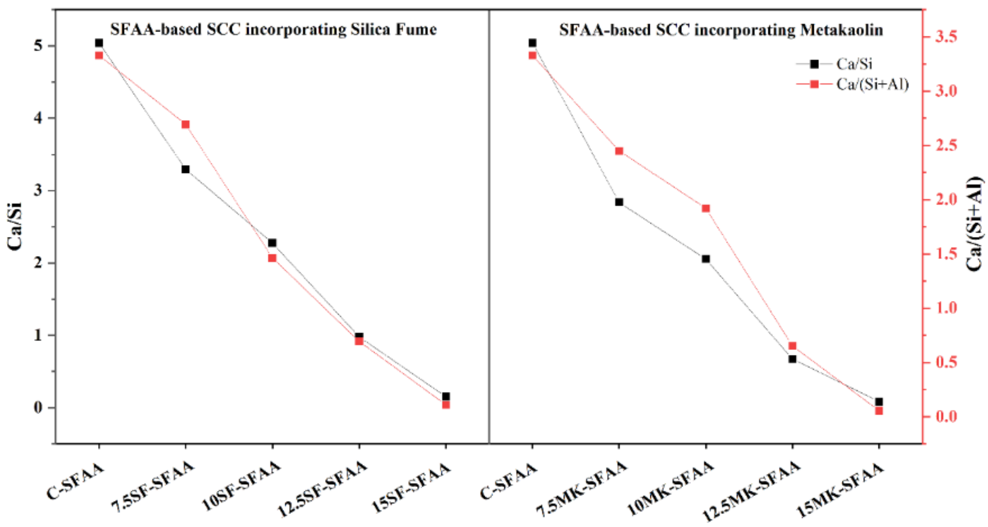

Figure 6. EDS analysis of SFAA-based SCC

5. CONCLUSIONS

The incorporation of SFAA provides an alternative utilisation route for fly ash while replacing natural coarse aggregates in self-compacting structural lightweight concrete. Although the present study did not include a direct environmental or life cycle assessment, the use of SFAA and SCMs may offer potential sustainability benefits through the utilisation of industrial by-products and reduced dependence on natural aggregate resources. The SFAA were pre-soaked to achieve an SSD condition, and the mixing water was adjusted according to their water absorption capacity to ensure consistent fresh-state performance. The developed mixtures achieved compressive strengths exceeding 60 MPa after 90 days, and the strength development was further validated through rebound hammer and UPV tests, demonstrating the suitability of the proposed lightweight SCC mixtures for structural applications.

Acknowledgment

The authors acknowledge the financial assistance from a fellowship to the first author by the Ministry of Education, New Delhi, India.

Data Availability Statement

Some or all data, models, or codes that support the findings of this study are available from the corresponding author upon reasonable request.

References

[1] Ankur, N., & Singh, N. (2024a). Strength characterization and sustainability assessment of coal bottom ash concrete. In *Environmental Science and Pollution Research* (Number 0123456789). Springer Berlin Heidelberg. https://doi.org/10.1007/s11356-024-33303-z

[2] Ankur, N., & Singh, N. (2024b). Valorisation of bottom ash in concrete: serviceability, microstructural and sustainability characterisation. *Magazine of Concrete Research*, *76*(21), 1241–1265. https://doi.org/10.1680/jmacr.23.00313

[3] Ankur, N., & Singh, N. (2026a). Coal Bottom Ash Concrete under Extreme Exposure Conditions: A Sustainable Solution for Environmental Protection. *Journal of Materials Engineering and Performance*. https://doi.org/10.1007/s11665-026-14085-6

[4] Ankur, N., & Singh, N. (2026b). Permeation, Toxicity, and Sustainability Assessment of Thermal Coal-Residue Concrete. *Journal of Materials in Civil Engineering*, *38*(2). https://doi.org/10.1061/JMCEE7.MTENG-21661

[5] Gökçe, H. S., Hatungimana, D., & Ramyar, K. (2019). Effect of fly ash and silica fume on hardened properties of foam concrete. *Construction and Building Materials*, *194*, 1–11. https://doi.org/10.1016/j.conbuildmat.2018.11.036

[6] Güneyisi, E., Gesoğlu, M., Karaoğlu, S., & Mermerdaş, K. (2012). Strength, permeability and shrinkage cracking of silica fume and metakaolin concretes. *Construction and Building Materials*, *34*, 120–130. https://doi.org/10.1016/j.conbuildmat.2012.02.017

[7] IS 516 Part 1/Sec 1. (2021). Hardened Concrete — Methods of Test Part 1 Testing of Strength of Hardened Concrete. *BUREAU OF INDIAN STANDARDS*.

[8] Kumar, P., Dinakar, P., & Saravanan, T. J. (2024a). *Development and Mechanical Performance of Self-Compacting Lightweight Aggregate Concrete Using Sintered Fly Ash Aggregates*. *36*(7). https://doi.org/10.1061/JMCEE7.MTENG-17831

[9] Kumar, P., Dinakar, P., & Saravanan, T. J. (2024b). *Development and Mechanical Performance of Self-Compacting Lightweight Aggregate Concrete Using Sintered Fly Ash Aggregates*. *36*(7). https://doi.org/10.1061/JMCEE7.MTENG-17831

[10] Kumar, P., Dinakar, P., & Saravanan, T. J. (2025). Development and performance analysis of structural lightweight aggregate self-compacting concrete: A sustainable solution. *Process Safety and Environmental Protection*, *197*(February), 107052. https://doi.org/10.1016/j.psep.2025.107052

[11] Kumar, P., Pasla, D., & Saravanan, T. J. (2023a). Self-compacting lightweight aggregate concrete and its properties : A review. *Construction and Building Materials*, *375*(February), 130861. https://doi.org/10.1016/j.conbuildmat.2023.130861

[12] Kumar, P., Pasla, D., & Saravanan, T. J. (2023b). Self-compacting lightweight aggregate concrete and its properties : A review. *Construction and Building Materials*, *375*(February), 130861. https://doi.org/10.1016/j.conbuildmat.2023.130861

[13] Kumar, P., Pasla, D., & Thiyagarajan, J. S. (2025). Synergetic effect of coarse sintered fly ash aggregates and supplementary cementitious materials in self-compacting concrete: From durability and corrosion perspective. *Journal of Building Engineering*, *108*(January), 112969. https://doi.org/10.1016/j.jobe.2025.112969

[14] Kumar, P., & Singh, N. (2023). Performance of recycled concrete aggregates based self-compacting concrete containing coal combustion ashes and silica fume. *European Journal of Environmental and Civil Engineering*, *0*(0), 1–26. https://doi.org/10.1080/19648189.2023.2293816

[15] Mermerdaş, K., Gesoğlu, M., Güneyisi, E., & Özturan, T. (2012). Strength development of concretes incorporated with metakaolin and different types of calcined kaolins. *Construction and Building Materials*, *37*, 766–774. https://doi.org/10.1016/j.conbuildmat.2012.07.077

[16] Nadesan, M. S., & Dinakar, P. (2017). Structural concrete using sintered flyash lightweight aggregate: A review. *Construction and Building Materials*, *154*, 928–944. https://doi.org/10.1016/j.conbuildmat.2017.08.005

[17] Nadesan, M. S., & Pasala, D. (2018). Materials and methods of sintered flyash lightweight aggregate. *Indian Journal of Scientific Research*, *17*(2), 24–31.

[18] Naito, C., Fox, J., Bocchini, P., & Khazaali, M. (2020). Chloride migration characteristics and reliability of reinforced concrete highway structures in Pennsylvania. *Construction and Building Materials*, *231*, 117045. https://doi.org/10.1016/j.conbuildmat.2019.117045

[19] Rawat, R., & Pasla, D. (2024). Mix design of FA-GGBS based lightweight geopolymer concrete incorporating sintered fly ash aggregate as coarse aggregate. *Journal of Sustainable Cement-Based Materials*, *13* (8), 1164–1179. https://doi.org/10.1080/21650373.2024.2361266

[20] Tejas, S., & Pasla, D. (2023a). Assessment of mechanical and durability properties of composite cement-based recycled aggregate concrete. *Construction and Building Materials*, *387* (February 2023), 131620. https://doi.org/10.1016/j.conbuildmat.2023.131620

[21] Tejas, S., & Pasla, D. (2023b). Assessment of mechanical and durability properties of composite cement-based recycled aggregate concrete. *Construction and Building Materials*, *387* (May 2023), 131620. https://doi.org/10.1016/j.conbuildmat.2023.131620

Declaration of interests

The authors declare that they have no known competing financial interests or personal relationships that could have appeared to influence the work reported in this paper.